



**AFRL-RX-WP-TP-2011-4217**

**USE OF ADVANCED CHARACTERIZATION TECHNIQUES TO  
STUDY STRUCTURAL AND COMPOSITIONAL TRANSITIONS  
ACROSS SOLID STATE INTERFACES (Preprint)**

**J. Tiley  
Metals Branch  
Metals, Ceramics & NDE Division**

**G.B. Viswanathan  
UES Inc.**

**R. Srinivasan  
ExxonMobil Research and Engineering  
Company**

**H.L. Fraser  
The Ohio State University  
Department of Materials Science  
and Engineering**

**R. Banerjee, S. Nag, and J.Y. Hwang  
University of North Texas**

**JULY 2011**

**Approved for public release; distribution unlimited.**

*See additional restrictions described on inside pages*

**STINFO COPY**

**AIR FORCE RESEARCH LABORATORY  
MATERIALS AND MANUFACTURING DIRECTORATE  
WRIGHT-PATTERSON AIR FORCE BASE, OH 45433-7750  
AIR FORCE MATERIEL COMMAND  
UNITED STATES AIR FORCE**

REPORT DOCUMENTATION PAGE					Form Approved OMB No. 0704-0188	
<p>The public reporting burden for this collection of information is estimated to average 1 hour per response, including the time for reviewing instructions, existing data sources, gathering and maintaining the data needed, and completing and reviewing the collection of information. Send comments regarding this burden estimate or any other aspect of this collection of information, including suggestions for reducing this burden, to Department of Defense, Washington Headquarters Services, Directorate for Information Operations and Reports (0704-0188), 1215 Jefferson Davis Highway, Suite 1204, Arlington, VA 22202-4302. Respondents should be aware that notwithstanding any other provision of law, no person shall be subject to any penalty for failing to comply with a collection of information if it does not display a currently valid OMB control number. <b>PLEASE DO NOT RETURN YOUR FORM TO THE ABOVE ADDRESS.</b></p>						
1. REPORT DATE (DD-MM-YY) July 2011		2. REPORT TYPE Journal Article Preprint		3. DATES COVERED (From - To) 01 July 2011 – 01 July 2011		
4. TITLE AND SUBTITLE USE OF ADVANCED CHARACTERIZATION TECHNIQUES TO STUDY STRUCTURAL AND COMPOSITIONAL TRANSITIONS ACROSS SOLID STATE INTERFACES (Preprint)				5a. CONTRACT NUMBER FA8650-08-C-5226		
				5b. GRANT NUMBER		
				5c. PROGRAM ELEMENT NUMBER 62102F		
6. AUTHOR(S) J. Tiley (Metals, Ceramics & NDE Division, Metals Branch (AFRL/RXLM)) R. Srinivasan (ExxonMobil Research and Engineering Company) R. Banerjee, S. Nag, and J.Y. Hwang (University of North Texas) G.B. Viswanathan (UES Inc.) H.L. Fraser (The Ohio State University, Department of Materials Science and Engineering)				5d. PROJECT NUMBER 4349		
				5e. TASK NUMBER 00		
				5f. WORK UNIT NUMBER LM114100		
7. PERFORMING ORGANIZATION NAME(S) AND ADDRESS(ES)  Metals, Ceramics & NDE Division, Metals Branch (AFRL/RXLM) Materials and Manufacturing Directorate, Air Force Research Laboratory Wright-Patterson Air Force Base, OH 45433-7750 Air Force Materiel Command, United States Air Force				8. PERFORMING ORGANIZATION REPORT NUMBER AFRL-RX-WP-TP-2011-4217		
9. SPONSORING/MONITORING AGENCY NAME(S) AND ADDRESS(ES)  Air Force Research Laboratory Materials and Manufacturing Directorate Wright-Patterson Air Force Base, OH 45433-7750 Air Force Materiel Command United States Air Force				10. SPONSORING/MONITORING AGENCY ACRONYM(S) AFRL/RXLM		
				11. SPONSORING/MONITORING AGENCY REPORT NUMBER(S) AFRL-RX-WP-TP-2011-4217		
12. DISTRIBUTION/AVAILABILITY STATEMENT Approved for public release; distribution unlimited.						
13. SUPPLEMENTARY NOTES PAO case number 88ABW-2010-2930, cleared 02 June 2010. The U.S. Government is joint author of this work and has the right to use, modify, reproduce, release, perform, display, or disclose the work. Submitted to JOM. Document contains color.						
14. ABSTRACT The atomic-scale study of solid-solid interfaces in complex multi-phase multi-component systems is a challenging but important endeavor. This article highlights the coupling of recently developed advanced characterization techniques, such as high resolution scanning transmission electron microscopy (HRSTEM), carried out in an aberration-corrected microscope, and 3D atom probe (3DAP) tomography, to address the structural and compositional transition at the atomic scale across solid-solid interfaces, such as the $\gamma/\gamma'$ interface in Ni-base superalloys and the $\alpha/\beta$ interface in titanium alloys. Possible implications of such investigations of the interface on the understanding of physical and mechanical properties are discussed.						
15. SUBJECT TERMS Ni-base superalloys, 3D atom probe tomography, high resolution scanning transmission electron microscopy (HRSTEM)						
16. SECURITY CLASSIFICATION OF:			17. LIMITATION OF ABSTRACT: SAR	18. NUMBER OF PAGES 24	19a. NAME OF RESPONSIBLE PERSON (Monitor) Jaimie Tiley	
a. REPORT Unclassified	b. ABSTRACT Unclassified	c. THIS PAGE Unclassified			19b. TELEPHONE NUMBER (Include Area Code) N/A	

## Use of Advanced Characterization Techniques to Study Structural and Compositional Transitions Across Solid State Interfaces

R. Srinivasan, R. Banerjee\*, G.B. Viswanathan<sup>@</sup>, S. Nag\*, J.Y. Hwang\*, J. Tiley<sup>#</sup>, H.L. Fraser<sup>^</sup>

ExxonMobil Research and Engineering Company, Annandale NJ 08801

\* University of North Texas, Denton TX 76203

<sup>@</sup> UES Inc., Dayton OH 45432

<sup>#</sup> Air Force Research Laboratory, Dayton OH 45433

<sup>^</sup> Department of Materials Science and Engineering, The Ohio State University, Columbus OH 43210

### Abstract

The atomic-scale study of solid-solid interfaces in complex multi-phase multi-component systems is a challenging but important endeavor. This article highlights the coupling of recently developed advanced characterization techniques, such as high resolution scanning transmission electron microscopy (HRSTEM), carried out in an aberration-corrected microscope, and 3D atom probe (3DAP) tomography, to address the structural and compositional transition at the atomic scale across solid-solid interfaces, such as the  $\gamma/\gamma'$  interface in Ni-base superalloys and the  $\alpha/\beta$  interface in titanium alloys. Possible implications of such investigations of the interface on the understanding of physical and mechanical properties are discussed.

### Introduction

Interfaces are known to play an important role in determining macroscopic properties (e.g. mechanical, electrical, magnetic) in multiphase systems [1-2]. As material properties continue to be dictated increasingly through nanoscale structural features, the accurate characterization of interface structure and composition at the atomic scale, and its role in determining material performance, is becoming increasingly critical. The study of structure at the atomic scale has typically involved the use of High Resolution TEM (HRTEM) based techniques [3,4], which rely on the principle of phase contrast imaging

to identify position of atomic columns and structural defects. Recent advances in HRTEM and HRSTEM imaging have been enabled through the development of aberration correctors for the image as well as the electron probe [5-8], thus allowing for a more direct interpretation of atomic scale structure. Simultaneously, recent development in techniques such as 3D Atom Probe (3DAP) tomography have enabled truly detailed studies of compositional transitions at the nanoscale [9-12] across solid-solid interfaces in multiphase systems. These recent advances have dramatically reduced the traditional limitations associated with the use of experimental techniques such as HRSTEM and 3DAP Tomography, thus enabling a direct study of structural and compositional transition across solid-solid interfaces at the atomic scale.

The synergistic coupling of aberration-corrected HRSTEM and 3DAP Tomography, as applied to the study of solid-solid interfaces, is highlighted in this manuscript. While several examples exist in literature on the utilization of each technique individually, the ability to develop a more comprehensive understanding of interface structure and composition, and consequently a better picture of the underlying physical reality, is highlighted through two separate examples in this article: the  $\gamma/\gamma'$  interface in Ni-base superalloys and the  $\alpha/\beta$  interface at the early stages of  $\alpha$ -phase nucleation in  $\beta$ -Titanium alloys.

### **Exploring the $\gamma/\gamma'$ interface in Ni-base superalloys**

The morphology, size and distribution of the ordered  $\gamma'$  precipitates in the disordered  $\gamma$  matrix of Ni-base superalloys are directly responsible for the observed mechanical properties such as creep and high temperature strength [13-18]. Consequently, the microstructural stability as a function of aging has been a topic of significant study. Coarsening of the  $\gamma'$  phase, viz. growth of  $\gamma'$  precipitates as a function of aging

time and temperature [15,16,19,20] can directly impact the observed mechanical behavior [16,17]. Classical models to explain coarsening kinetics have been based upon the LSW model, which derives coarsening kinetics based upon a volume diffusion based coarsening mechanism [21, 22]. However, a more recent model, proposed by Ardell and Ozolins [23] argues that the coarsening kinetics could be controlled by diffusion of key element(s) across a partially ordered interface of finite width. Clearly, one of the fundamental factors responsible for the validity of either model remains the nature of the  $\gamma/\gamma'$  interface – existence of a partially ordered  $\gamma/\gamma'$  interface lends more credence to a interface diffusion-mediated mechanism of coarsening, and may in turn entail more profound implications for alloy design and chemistry. While the resolution associated with earlier techniques may have posed a limitation in the past, the utilization of advanced characterization techniques, such as aberration-corrected HRSTEM and 3DAP Tomography, offers the opportunity for detailed investigation of the  $\gamma/\gamma'$  interface at the atomic scale.

Rene'88 DT was chosen as a candidate material for this study, primarily due to the low lattice misfit between the  $\gamma$  and  $\gamma'$  phases ( $<0.05\%$ ), and the opportunity afforded to study compositional transitions in a complex multicomponent alloy (Rene'88 DT: 55.6Ni-18.02Cr-13Co-4.74Ti-4.45Al-2.48Mo-1.21W-0.46Nb in at.%). Samples subjected to a supersolvus annealing treatment (1150 C for 0.5h), followed by cooling to RT at 24 C/min, show the typical microstructure [15] of ordered  $L1_2$   $\gamma'$  precipitates in a disordered FCC  $\gamma$  matrix (Figure 1a) [24]. A more detailed discussion of the observed bimodal size distribution, effect of cooling rate and aging time on precipitate morphology and size evolution is presented elsewhere [19].

Atomic resolution, Z-contrast HAADF-HRSTEM imaging was performed in a FEI Titan 80-300 S/TEM, equipped with a probe aberration corrector, to study the interface between a secondary  $\gamma'$  precipitate and the  $\gamma$  matrix (see [24] for details on specimen preparation and imaging). In order to ensure consistency between the HRSTEM and 3DAP studies (discussed below), an interface orientation parallel to the  $\{002\}$  planes was specifically chosen. HRSTEM investigations reveal a non-abrupt  $\gamma/\gamma'$  interface (Figure 1b) – note the superlattice structure in the  $\gamma'$  phase (inset FFT-left) and lack of order in the  $\gamma$  phase (inset FFT-right). As shown in the higher magnification, filtered image in Figure 1c, the  $\gamma'$  phase, parallel to the  $\{002\}$  interface, shows alternating planes of pure Ni and Ni+Al sublattices (see Figure 1d), while the  $\gamma$  phase shows only a single sublattice. Averaged intensity plots from the  $\gamma'$  to the  $\gamma$  phase (intensity averaged across lines AB through CD in Figure 2a) show a clear transition region from the  $\gamma'$  to the  $\gamma$  phase (Figure 2b). In fact, a plot of neighboring intensity ratios (Figure 2c), which can be a qualitative estimate of a long-range order parameter, clearly show an order-disorder transition region (X1-X2, avg. value  $\sim 6$ -8  $\{002\}$  planes), and an overall compositional transition region (X1-X3, avg. value 12-14  $\{002\}$  planes), which encompasses the order-disorder transition (the reader is again referred to [24] for further details). Interestingly, the presence of heavier alloying elements is reflected in the higher background intensity observed in the  $\gamma$  matrix. Thus, a clear order-disorder, or structural, transition can be observed through HRSTEM investigations.

In order to study compositional transitions, as well as provide a complementary validation basis to the HRSTEM investigations, 3DAP Tomography was carried out on the same Rene'88 DT material. Figure 3a shows an iso-concentration plot of a prepared 3DAP specimen (refer [12,24] for details on specimen preparation), clearly showing a narrow  $\gamma$  channel (blue, Co-rich) between two secondary  $\gamma'$  precipitates (red, Al-rich). This is also confirmed in the Al-ion image shown in Figure 3b. Interestingly, the order in

the  $\gamma'$  phase is clearly observed in the higher magnification Al-ion image in Figure 3c, which suggests an order-disorder transition from the  $\gamma'$  to the  $\gamma$  phase over 3 Al {002} planes (6 {002} planes). Furthermore, a proximity histogram [25] across the indicated  $\gamma/\gamma'$  interface (Figure 3d) shows a clear compositional transition occurring over  $\sim 2$  nm ( $\sim 12$  {002} planes). Thus, the 3DAP investigations are in very good agreement with the HRSTEM observations, and the combined information from these advanced, complementary analytical techniques suggests a non-abrupt  $\gamma/\gamma'$  interface structure that consists of two distinct regions – an order-disorder transition width, and a compositional transition width. The non-abrupt nature of the interface, as experimentally observed through these advanced characterization techniques, implies that the possibility of coarsening being controlled through diffusivity across a partially ordered  $\gamma/\gamma'$  interface cannot be ignored. While further studies are required for conclusive proof, it is interesting to note that recent simulation as well as experimental studies have indicated that the diffusion of Al (a key order-disorder determining element) across the partially ordered  $\gamma/\gamma'$  interface, could indeed be a possible rate-controlling step in the coarsening process [19,23].

Remarkably, recent results on atomistic modeling of the  $\gamma/\gamma'$  interface in the binary Ni-Al system [23, 26] predict a non-abrupt interface. In fact, Mishin's results on the Ni/Ni<sub>3</sub>Al interface [26] indicate that the transition from  $\gamma'$  to  $\gamma$  (measured as a variation of the Al-sublattice occupancy) can occur over 4-6 {002} layers, again in very good agreement with the experimental observations. Clearly, these correlations between the experimental observations and atomistic modeling are encouraging; however it should be noted that other recent studies have indicated that the  $\gamma/\gamma'$  interface structure is also a function of the precipitate morphology, type (i.e. secondary vs. tertiary) and aging parameters [27-29]. Nevertheless, the observations do provide valuable insight into factors that may govern  $\gamma'$  coarsening, and more importantly, raise fundamental questions regarding the definition of an order-disorder interface, or more generally,

interfaces in multiphase multicomponent systems. Such atomic-scale knowledge of structure and composition, essential for a fundamental, physics-based understanding of complex solid-solid interfaces, can only be enhanced through utilization of complementary advanced characterization techniques available today.

### **$\alpha/\beta$ interfaces at the early stages of $\alpha$ nucleation in the $\beta$ matrix of titanium alloys**

This section of the article focuses on  $\alpha$  precipitation in a commercial  $\beta$  titanium alloy, the alloy Ti-5Al-5Mo-5V-3Cr-0.5Fe (in wt%), commonly referred to as Ti-5553, expected to be applicable for thick section aerospace components due to its high strength, reported to be as high as 1250 MPa at room temperature for certain microstructures, and its deep-hardenability [30-33] over larger thicknesses ( $\sim 150$  mm). Depending on the microstructure, this alloy can exhibit room temperature strengths as high as 1138 - 1172 MPa (UTS) while retaining useful ductility and toughness. However, it is important to note that the properties of Ti-5553 can vary over a wide range and are critically dependent on the microstructure, warranting a detailed investigation of the volume fraction, size, morphology and distribution of  $\alpha$  precipitates within the  $\beta$  matrix [34,35]. By varying the temperatures, times and cooling rates in individual heat-treatments, it is possible to vary the volume fraction and morphology of the  $\alpha$  phase nucleated within the  $\beta$  matrix phase in this alloy. The partitioning of the alloying elements, Al, V, Mo, Cr, and, Fe, also depends on the heat-treatments influenced by the alloy. Therefore, a critical study of the structural and compositional transitions across the  $\alpha/\beta$  interfaces in this alloy, as a function of heat-treatment is essential for the development of mechanistic models relating microstructure to mechanical properties.

The nucleation sites for the  $\alpha$  phase within the  $\beta$  phase of  $\beta$ -Ti alloys include, prior  $\beta$  grain boundaries,  $\beta/\omega$  interfaces,  $\beta/\beta'$  interfaces, and other defects such as dislocations and intermetallic particles within the



matrix [36]. Depending on the overall composition of the  $\beta$  titanium alloy and the specific heat-treatment experienced by the alloy, these different sites may or may not play a substantial role in  $\alpha$  nucleation. In case of the Ti-5553 alloy, recent experimental investigations have clearly shown the role of  $\omega$  precipitates on the nucleation of  $\alpha$  [37]. Thus, after solutionizing in the high temperature single  $\beta$  phase field and water-quenching to room temperature, Ti-5553 exhibited a homogeneous distribution of nanoscale  $\omega$  precipitates. Subsequent isothermal annealing at 350°C for 2 hours resulted in the growth and coarsening of these  $\omega$  precipitates accompanied with the nucleation of  $\alpha$  platelets. These  $\alpha$  precipitates were found to nucleate either at the  $\beta/\omega$  interfaces or in close proximity to the  $\omega$  precipitates suggesting an  $\omega$ -assisted nucleation mechanism for the  $\alpha$  precipitates [37]. A dark-field TEM micrograph, recorded with the objective aperture encompassing diffraction spots from both the co-existing  $\alpha$  and  $\omega$  phases, is shown in Figure 4a. While these  $\alpha$  precipitates exhibit a lenticular morphology, the  $\omega$  precipitates exhibit a more ellipsoidal morphology.

Subsequent isothermal annealing at 400°C for 2 hours resulted in two changes, namely, growth and coarsening of the lenticular  $\alpha$  precipitates and the complete dissolution of the  $\omega$  precipitates. Thus, it can be inferred that the  $\omega$ -solvus temperature for Ti-5553 lies in the range of 350-400°C. Figure 4b shows a dark-field TEM image from this 400°C annealed Ti-5553 sample, clearly exhibiting the coarsened  $\alpha$  precipitates. HRTEM (phase contrast) imaging studies on the nanometer scale lenticular  $\alpha$  precipitates and their interface with the surrounding  $\beta$  matrix were carried out in the FEI TITAN S/TEM. Figure 4c shows a near-Scherzer HRTEM image of a  $\langle 110 \rangle$  oriented  $\beta$  grain containing two  $\langle 0001 \rangle$  oriented  $\alpha$  precipitates. The  $\alpha$  precipitates exhibit a well-developed *hcp* crystal structure with distinct ledges visible at the  $\alpha/\beta$  interfaces for both precipitates. A Fourier transform from this region, clearly showing spots

from the  $\langle 0001 \rangle$  zone axis of the Burgers oriented  $\alpha$  precipitates, parallel to the  $\langle 110 \rangle$   $\beta$  zone axis, has been included as an inset in Figure 4c.

A higher magnification view of the atomic-scale structural details of the  $\alpha/\beta$  interface is shown in Figure 5a. The *hcp* structure is well-developed on the  $\alpha$  side of the interface and an atomistically-sharp interface with ledges is clearly visible. The compositional partitioning between the  $\alpha$  and  $\beta$  phases on aging Ti-5553 at 400°C has also been determined using 3D atom probe (3DAP) tomography studies. It should be noted that the complexity of this alloy in terms of the number of alloying elements (5 in case of Ti-5553) coupled with the nanometer size scale of the  $\alpha$  precipitates, in the early stages of precipitation, makes these measurements rather challenging and beyond the scope of most other characterization techniques. Furthermore, using the LEAP microscope it is now possible to sample a substantially larger volume of material compared with more traditional atom probe tomography instruments. In order to determine the composition of these  $\alpha$  precipitates, the composition profiles of the constituent elements are averaged over a cylinder of diameter 5 nm in a 60nm X 60nm X 25nm volume 3DAP reconstruction, shown in Figure 5b. The regions exhibiting a higher concentration of Al ions (blue) in Figure 5b correspond to the  $\alpha$  precipitates while the regions in between exhibit a higher concentration of V (red) and Cr (yellow) ions corresponding to the  $\beta$  regions. The actual composition profiles for Al in blue and V in red are shown in Figure 5c [37]. In addition, the regions corresponding to  $\alpha$  and  $\beta$  phases have also been specifically marked on the composition profiles in Figure 5c. From these compositional profiles it is evident that the  $\alpha$  regions exhibit depletion of the  $\beta$  stabilizers, such as V and an enrichment of Al. The average Al concentration within the  $\alpha$  phase in this case is  $\sim 14$  at%. Overall the compositional partitioning between the  $\alpha$  and  $\beta$  phase at this early stage of precipitation is not substantial. Based on the compositional profile, the average composition of  $\alpha$  precipitates at this stage appears to be Ti-13.5Al-3V-2Mo-2Cr-1Fe (all in

at%) whereas that of the retained  $\beta$  matrix appears to be Ti-10Al-6.5V-4Mo-6Cr-1Fe (all in at%). The error bars associated with the compositional profiles for Al and V shown have also been marked in Figure 5c. These errors have been calculated based on the statistical errors associated with 3DAP measurements [38] and indicate that while the Al enrichment in the  $\alpha$  precipitates is marginal, it still appears to be statistically significant. Moreover, it is important to note that while the composition of these  $\alpha$  precipitates is far-from equilibrium, they exhibit a fully developed *hcp* structure with sharp  $\alpha/\beta$  interfaces and a Burgers orientation relationship with the  $\beta$  matrix. These findings are significant with respect to understanding the mechanism of nucleation and growth of the  $\alpha$  phase in the  $\beta$  matrix of  $\beta$ -Ti alloys, as they suggest that a nucleation and growth could indeed occur by a mixed-mode displacive-diffusive transformation, much like the bainitic transformation in steels [39] and Al-Ag alloys [40].

### **Summary Remarks, Current Limitations, and Future Directions**

Solid-solid interfaces play a dominant role in determining physical, chemical, and, mechanical properties of many materials systems, especially those involving complex multi-phase microstructures. Therefore the characterization of these interfaces across multiple length scales is absolutely critical for the development of robust physically-based models relating the microstructure to the properties. With the recent advances in characterization techniques such as aberration-corrected high-resolution scanning transmission electron microscopy (HRSTEM) and three-dimensional atom probe (3DAP) tomography, it is now possible to characterize structure and composition of interfaces at true atomic scales. It is important to reiterate the complementary nature of these new techniques and the consequent ability to couple information from such independent techniques when applied to the same problem, resulting in an atomic scale rendition of the interface, closer to the physical reality than possible ever before. This opens up tremendous opportunities in terms of characterizing complex solid-solid interfaces at unprecedented spatial and compositional

resolutions and can be applied to a broad spectrum of materials including metals and alloys, ceramics, electronic materials, and, composites or hybrid materials. Despite these advances there still exist critical limitations in terms of these techniques that need to be addressed. **(Hamish, please add a few sentences on limitations and future directions – your perspectives from the Hawaii workshop?).**

## References

1. H. Yamada et al, Science 305 (2004), pp.646
2. A. Ziegler et al, Science 306 (2004), pp.1768
3. C.L. Jia, M. Lentzen, K. Urban, Science 299 (2003), pp. 870
4. C.L. Jia, K. Urban, Science 303 (2004), pp. 2001
5. D.A. Muller et al, Nature 399 (1999), pp. 758
6. H. Muller, S. Uhlemann, P. Hartel, M. Haider, Microsc. Microanal. 12 (2006), 442
7. M. Haider, S. Uhlemann, J. Zach, Ultramicroscopy 81 (2000), 163
8. H. Rose, Ultramicroscopy 103 (2005), 1
9. M.K. Miller, Micron 32 (2001), pp. 757
10. D. Blavette, L. Letellier, A. Raccine, A. Hazotte, Microsc. Microanal. Microstruct. 7 (1996), 185
11. K.E. Yoon, D. Isheim, R.D. Noebe, D.N. Seidman, Interface Sci. 9 (2001), 249
12. J. Hwang, R. Banerjee, J. Tiley, R. Srinivasan, G.B. Viswanathan, H.L. Fraser, Mater. Trans. A 40A (2009), pp. 24
13. D.D. Krueger, R.D. Kissinger, R.D. Menzies, C.S. Wukusick, U.S. Patent 4957567 (1990).
14. D.D. Krueger, R.D. Kissinger, R.D. Menzies, in Superalloys 1992, eds. S.D. Antolovich et al., TMS-AIME, Warrendale PA (1992), pp. 277
15. S.T. Wlodek, M. Kelly, D.A. Alden, in Superalloys 1996, eds. R.D. Kissinger et al., TMS, Warrendale PA (1996), pp. 129
16. G.B. Viswanathan, P.M. Sarosi, D.D. Whitis, M.J. Mills, Acta Mater. 53 (2005), pp. 3041
17. S.K. Sondhi, B.F. Dyson, M. McLean, Acta Mater. 52 (2000), pp. 1761
18. Gornostyrev, O.Y. Kontsevoi, K.Y. Khromov, M.I. Katsnelson, A.J. Freeman, Scripta Mater. 56 (2007), 81
19. J. Tiley, G.B. Viswanathan, R. Srinivasan, R. Banerjee, J. Hwang, D.M. Dimiduk, H.L. Fraser, Acta Mater. 57 (2009), pp. 2538
20. J. Tiley, R. Srinivasan, R. Banerjee, G.B. Viswanathan, B. Toby, H.L. Fraser, Mater. Sci. Tech. 25 (2009), pp. 1369-1374
21. I.M. Lifshitz, V.V. Sil'ozov, J. Phys. Chem. Solids 19 (1961), pp. 35
22. C. Wagner, Z. Elektrochem 65 (1961), pp. 581
23. A.J. Ardell, V. Ozolins, Nat. Mater. 4 (2005), pp. 309
24. R. Srinivasan, R. Banerjee, J.Y. Hwang, G.B. Viswanathan, J. Tiley, D.M. Dimiduk, H.L. Fraser, Phys. Rev. Lett. 102 (2009), pp. 086101
25. O.C. Hellman et al, Microsc. Microanal. 6 (2000), pp. 437
26. Y. Mishin, Acta Mater. 52 (2004), pp. 1451
27. K.E. Yoon, R.D. Noebe, O.C. Hellman, D.N. Seidman, Surf. Interface. Anal. 36 (2004), 594
28. J.Y. Hwang, S. Nag, A.R.P. Singh, R. Srinivasan, J. Tiley, H.L. Fraser, R. Banerjee, Scripta Mater. 61 (2009), pp. 92-95
29. J.Y. Hwang, S. Nag, A.R.P. Singh, R. Srinivasan, J. Tiley, G.B. Viswanathan, H.L. Fraser, R. Banerjee, Mater. Trans. 40A (2009), pp. 3059-3068
30. S. Veeck, D. Lee, R. Boyer, and, R. Briggs, J. Adv. Mater. 37 (2005), pp. 40.
31. N.Clement, A. Lenain and P.J. Jacques, JOM, 59 (2007), pp. 50.
32. V.N. Moiseev in Titanium '95: Science and Technology, eds.: P.A. Blenkinsop, W. J. Evans, H.M. Flower, The Institute of Materials, London, England (1996), pp.1387.

33. C. Roubaud, T. Grosdidier, M. Phillippe, Y. Combres in Titanium '95: Science and Technology, eds.: P.A. Blenkinsop, W. J. Evans, H.M. Flower, The Institute of Materials, London, England (1996), pp.996.
34. V.V. Shevel'kov, Translated from Metallovedenie i Termicheskaya Obrabotka Metallov, 8 (1992), pp.33-37.
35. J.C Fanning, J. Mat. Eng. Perf., 14 (2005), pp.788-791.
36. T.W. Duerig, and, J.C. Williams, Beta Titanium alloys in the 80's: Proceedings of the Symposium, Atlanta, GA, United States (1984), pp.19-67.
37. S. Nag, R. Banerjee, R. Srinivasan, J. Y. Hwang. M. Harper, and, H. L. Fraser, Acta Mater. 57 (2009), pp.2136.
38. M. K. Miller, "Atom Probe Tomography: Analysis at the atomic level", Springer, ed.1 (2000).
39. H.D.K.H. Bhadeshia, J.W. Christian, Metall. Trans. A, 21A (1990), pp. 767.
40. B.M. Muddle, J.F. Nie, Scripta mater. 47 (2002), pp. 187.

## Figure Captions

Figure 1: (a) Cr-M EFTEM image showing the morphology and dispersion of ordered  $\gamma'$  precipitates in the  $\gamma$  matrix of Rene 88 DT. Larger secondary  $\gamma'$  and smaller tertiary  $\gamma'$  precipitates are visible, (b) HRSTEM image along the [100] zone showing the interface between a secondary  $\gamma'$  precipitate and  $\gamma$  matrix, insets show FFT's in the respective phases, (c) higher magnification filtered HRSTEM image showing the structural and compositional transition across the  $\gamma/\gamma'$  interface, (d) schematic diagram of the  $\gamma$  and  $\gamma'$  unit cells, with the (002) plane indicated.

Figure 2: (a) HRSTEM image from the box ABCD delineated in Figure 1(c). (b) Averaged intensity profiles across row AB through CD showing transition from ordered  $\gamma'$  to disordered  $\gamma$ , (c) Progressive intensity ratios showing the order-disorder transition and compositional width of the interface.

Figure 3: Al 10% (red) and Co 19% (blue) isosurfaces depicting morphology of the  $\gamma'$  precipitate used in 3DAP analysis; the red area is indicative of the secondary  $\gamma'$  precipitate, (b) and (c) higher magnification Al-ion images showing stacking of alternate Al (002) planes in the  $\gamma'$  phase, (d) Proxigram depicting compositional transition across the  $\gamma/\gamma'$  interface indicated by arrow in the inset.

Figure 4: (a) Dark field TEM image recorded using the  $\omega$  and  $\alpha$  reflections at the  $\langle 113 \rangle \beta$  zone in Ti-5553 aged 2h at 350 C and water quenched. Inset shows a lenticular  $\alpha$  precipitate nucleating on an  $\omega$  precipitate, (b) Dark Field TEM image recorded in Ti-5553 aged 2h at 400 C and water quenched, showing profuse nucleation and growth of lenticular  $\alpha$  precipitates. The  $\omega$  phase is absent, indicating that the  $\omega$  solvus temperature lies between 350 C and 400 C in this alloy, (c) near-Scherzer HRTEM image along  $\langle 0001 \rangle \alpha \parallel \langle 110 \rangle \beta$  showing the well-developed ledges along the a/b interface in Ti-5553 aged 2h at 400 C and water quenched.

Figure 5: (a) Higher magnification HRTEM image showing the  $\alpha/\beta$  interface structure from Figure 4(c), (b) 3DAP reconstruction of Al (blue), V (red) and Cr (yellow) atoms from Ti-5553 aged 2h at 400 C, showing  $\alpha$  and  $\beta$  regions, (c) Al and V composition profiles with statistical error bars from 5nm dia. cylinder indicated in (b), showing compositional transitions between  $\alpha$  and  $\beta$  phases.

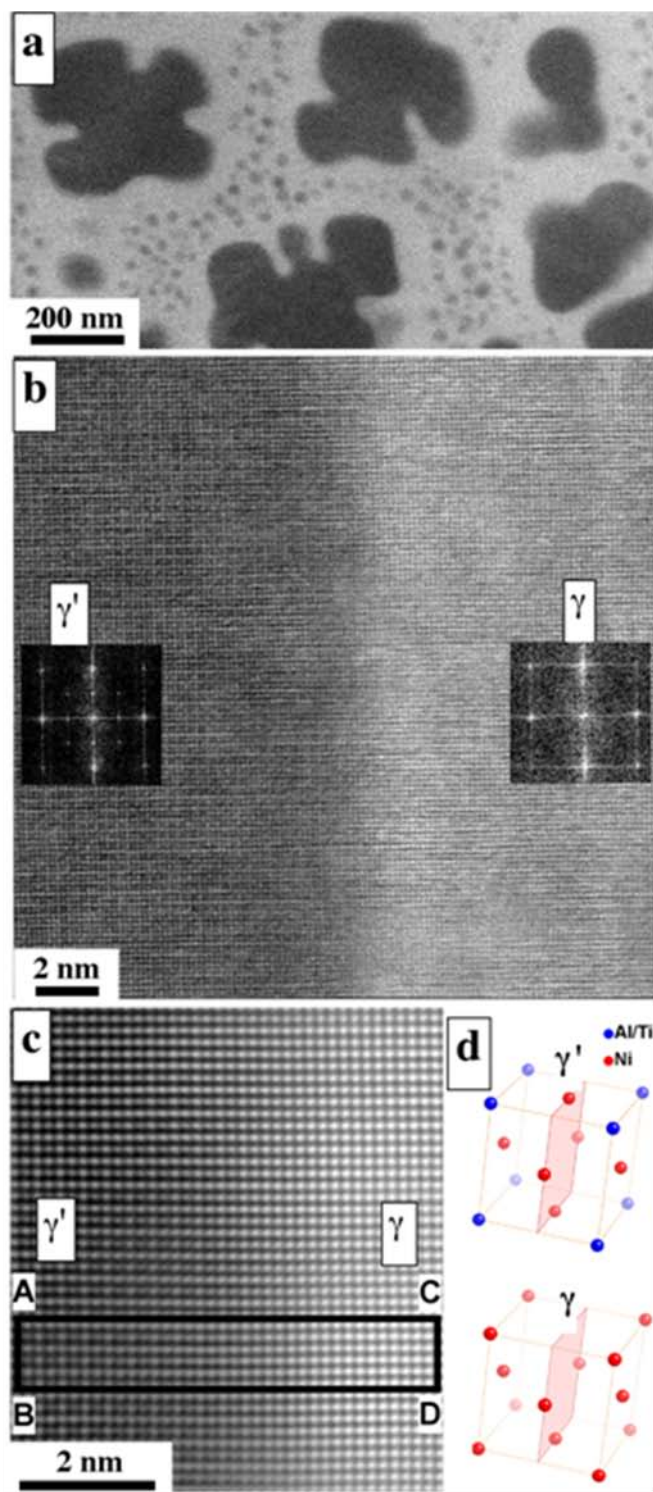


Figure 1

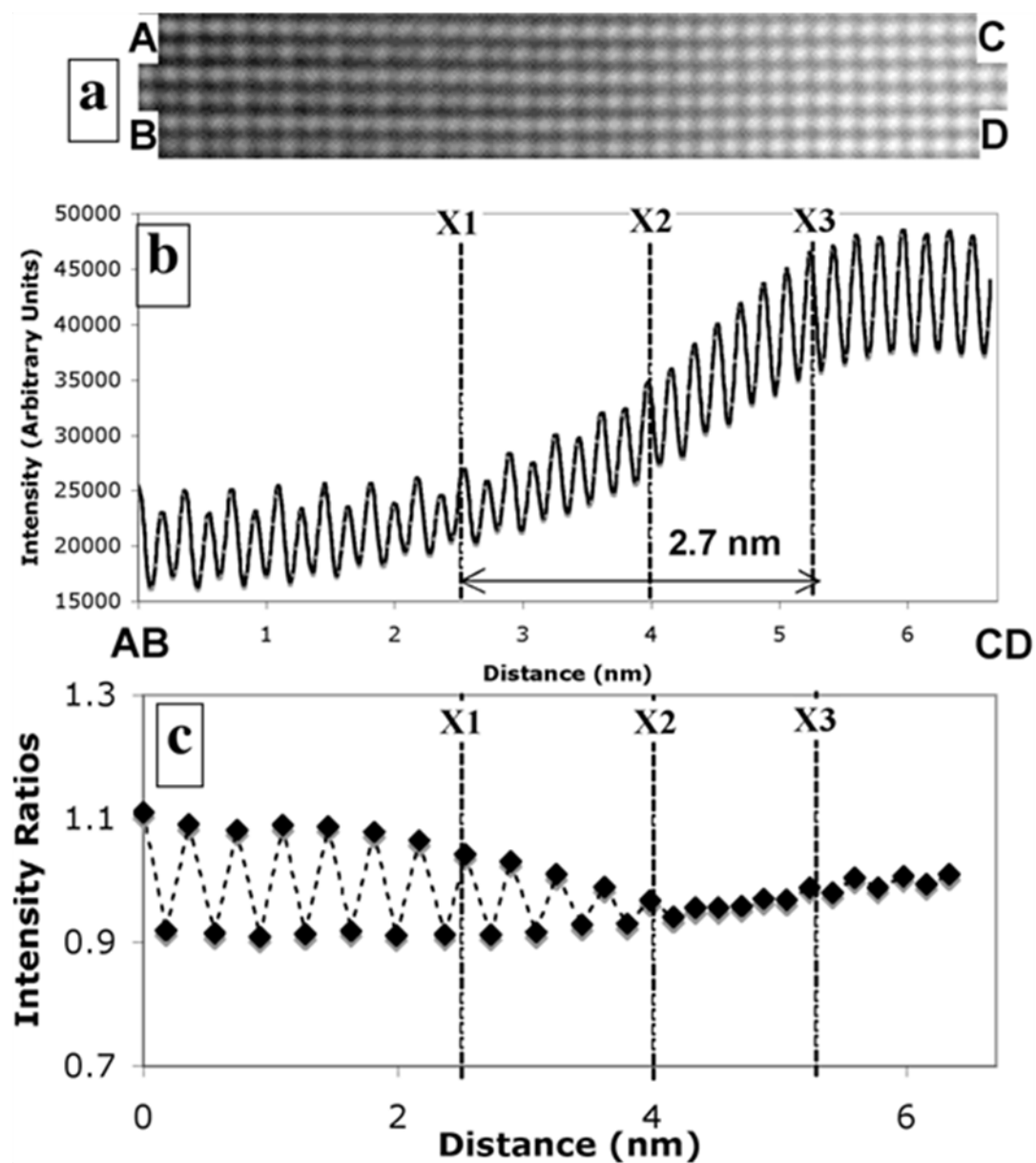


Figure 2



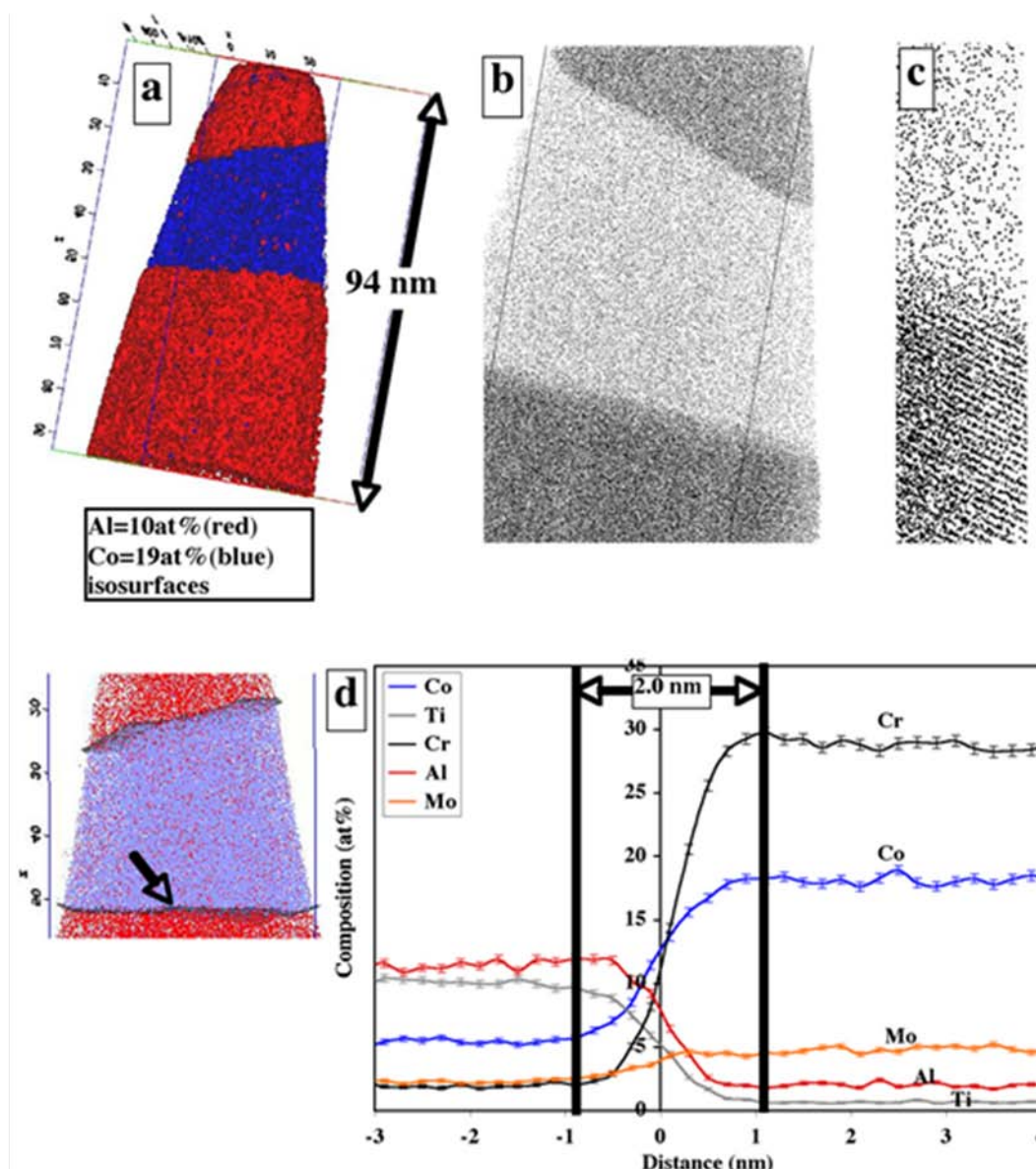


Figure 3

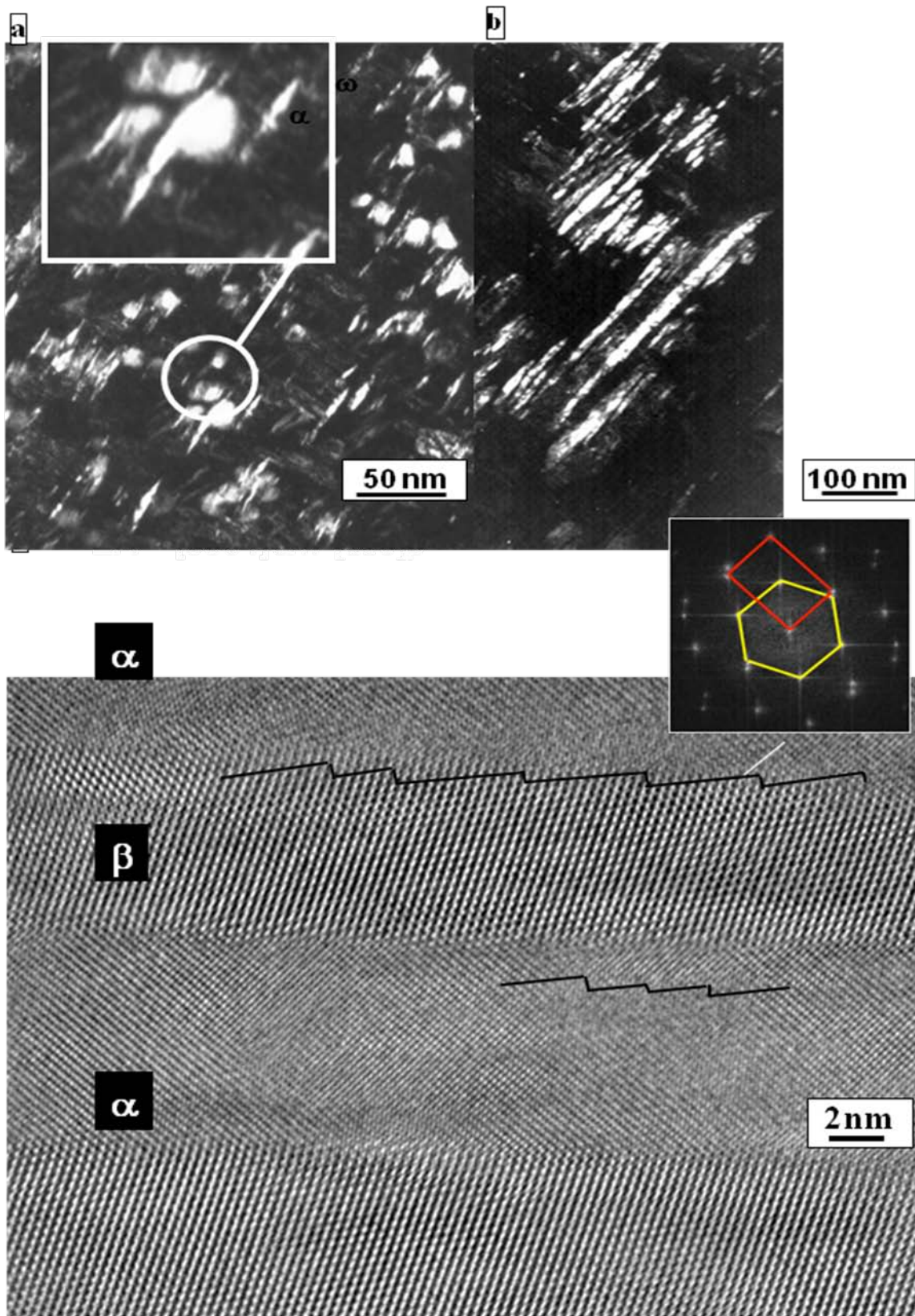


Figure 4

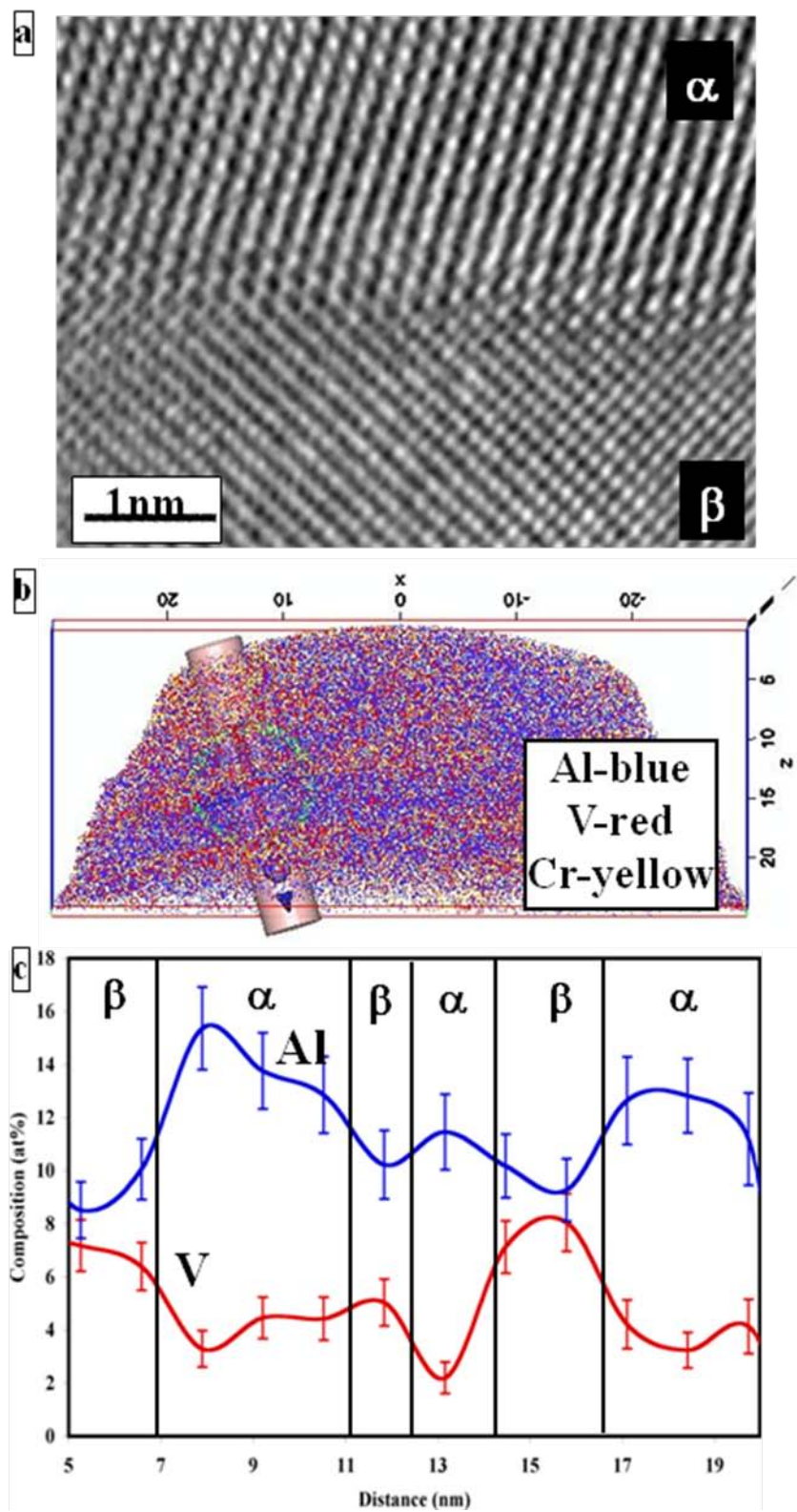


Figure 5